

# Difference Analysis of Antifibrin Images in the Detection of Deep Venous Thrombosis

Bruce R. Line and Paul H. Neumann

Department of Radiology, Albany Medical Center, Albany, New York

This study was designed to test the hypothesis that the detection of non-blood-pool localization due to deep venous thrombosis uptake can be enhanced by computer processing.

**Methods:** Immediate blood-pool and 90-min delay images from 25 patient studies obtained with  $^{99m}\text{Tc}$  T2G1s antifibrin were paired into 125 image sets (5/pt, including A, P knees, A, P calves and A thighs). After spatially aligning the image pairs, the blood-pool activity obtained from the immediate image was removed from the delayed image to produce a "clot only" image. Unprocessed data (UnP) and computer processed images (CmP) were presented to novice readers as part of a receiver operator characteristic (ROC) comparison study. The image interpreters were asked to provide independent diagnostic assessment at 250 limb sites using both datasets. Image intensity and color scale mappings were freely adjustable. Three readers were presented with images adjusted with optimal image contrast as judged by an observer with knowledge of the correct response. **Results:** The area under the ROC curve (Az), a measure of the method's accuracy, for these readers was 88.5% (UnP) and 88.8% (CmP) ( $p = \text{ns}$ ). Four readers whose images were not optimized showed Az of 79.1% (UnP) and 90.7% (CmP) ( $p < 0.05$ ). Average diagnostic decision time for all readers, per limb site, was  $18.2 \pm 7.8$  sec,  $m \pm \text{s.e.m.}$ , (UnP) and  $7.6 \pm 4.6$  sec (CmP). **Conclusion:** Novice reader accuracy is improved with computer processed images when image intensity and contrast factors are important. Computer processing can provide "clot" images that minimize nonspecific blood background activity and allow greater interpreter decision speed/confidence.

**Key Words:** venography; scintigraphy; deep venous thrombosis; computer analysis

J Nucl Med 1995; 36:2326-2332

**T**hromboemboli cause or contribute to 200,000 deaths per year in the U.S. (1), the majority of which arise in the deep iliofemoral veins (2). The venogram is considered the most accurate means of detecting extremity thrombotic disease. It may be used to evaluate the entire lower extremity deep venous system, including the calf and pelvic veins.

Unfortunately, contrast venography is an invasive procedure and there is a low but definite risk of both nephrotoxicity and anaphalactoid reaction to iodinated contrast agents.

Radiolabeled monoclonal antibodies that bind to either fibrin or to platelet deposits may provide an alternate imaging technology that is highly specific and sensitive for thromboembolic disease (3). T2G1s Fab' antifibrin antibody is directed against an epitope on fibrin in newly-formed, acute venous thrombi (4). The diagnostic sensitivity and specificity of  $^{99m}\text{Tc}$  T2G1s Fab' scintigraphy for proximal deep venous thrombosis (DVT) is 79% and 91%, respectively (5). Multicenter trials have shown antifibrin scintigraphy to be technically uncomplicated, safe, specific for acute thrombus and useful for the entire lower extremity, including calf and pelvic veins (5).

Tracer localization in thrombus allows it to be differentiated from nonspecific blood-pool activity that tends to fall over time due to renal clearance. Thus, visual clot detection involves a series of comparisons and decisions regarding differential uptake and clearance in vascular regions. This process can be tedious, especially where the vascular detail is complex. We postulated that differential uptake analysis should reduce the number of interpretation decisions, thereby increasing both interpretation speed and accuracy. To test this hypothesis, we presented readers with separate sets of unprocessed and processed images and compared their interpretations with independent venogram results. We report the relative performance of novice readers using receiver operating characteristic methods.

## MATERIALS AND METHODS

### Patient Scan Data and Venography

Preclinical studies have shown a 4-hr blood-pool half-life for  $^{99m}\text{Tc}$ -T2G1s Fab' (6) and no adverse effects of heparin on thrombus uptake (7). A large prospective multicenter trial was carried out in the United States and Europe to evaluate the diagnostic performance of  $^{99m}\text{Tc}$  antifibrin ( $^{99m}\text{Tc}$ -T2G1s Fab') in patients with suspected acute DVT (8). In the trial, over 500 patients received 0.5 mg T2G1s labeled with 15-20 mCi  $^{99m}\text{Tc}$ . Planar images were obtained with a large field of view gamma camera using either high-resolution or general-purpose collimation. Images were acquired immediately following injection to establish the blood-pool distribution of the antibody and then again at 90 min and 4 to 6 hr postinjection. From this population of patients, 25

Received Oct. 25, 1994; revision accepted Mar. 6, 1995.

For correspondence or reprints contact: Bruce R. Line, MD, Professor of Radiology, Nuclear Medicine, A-72, Albany Medical Center, Albany, NY 12208.

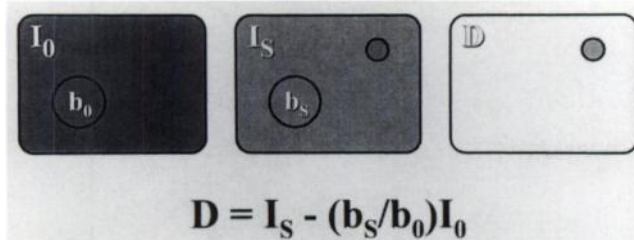


**FIGURE 1.** Concept schematic of difference analysis. The fractional change in blood-pool activity ( $\beta_s/\beta_0$ ) between an initial image ( $I_0$ ) and a subsequent image ( $I_s$ ) is used to generate an image of blood-pool activity at the subsequent time ( $(\beta_s/\beta_0) \cdot I_0$ ). This predicted image is then subtracted from the subsequent image to yield a difference image ( $D$ ) that reflects non-blood-pool sources of activity. The regions of interest,  $\beta_0$  and  $\beta_s$ , are placed over vascular areas that are primarily blood pool. A clot represented as a region in the upper right of the  $I_s$  image does not follow the fractional change kinetic of the blood and is enhanced in the difference image.

were selected for inclusion in the test set. Twelve studies were included because they were considered illustrative of well-defined normal or abnormal cases. The remaining studies were challenging, each of which was missed by an expert panel of nuclear medicine clinicians who interpreted all of the multicenter trial studies. The test cases were obtained from the sponsor of the multicenter trial in digital,  $128 \times 128$  byte mode images.

Contrast venography was performed within 24–36 hr of acquisition of the antifibrin images. All venogram data on these patients were interpreted by two consulting radiologists whose readings were accepted when concordant and otherwise were adjudicated by a third independent reading. Venograms were interpreted by calf, knee or thigh limb site and were read as locally positive, negative or indeterminate for the presence of thrombus.

### Difference Algorithm

In T2G1s Fab' scintigraphy, image background falls with time due to renal clearance of blood-pool tracer. Hence, regions having kinetics different from those expected for blood pool may contain tissue having different, possibly pathologic, physiology. The equations in the Appendix describe the manipulations used to produce an image of the non-blood-pool compartments of a T2G1s antifibrin data set. The basic premise is illustrated in Figure 1. An image obtained immediately after intravenous tracer injection ( $I_0$ ) reflects the blood pool; the tracer has neither moved extravascularly nor combined with a clot target to an appreciable extent. In an image obtained at some subsequent time ( $I_s$ ), the blood pool has decreased in activity due to clearance through the kidneys and transvascular leak. Since the blood pool is a single compartment, there is an equal fractional change in the blood activity in all image regions. The fractional change ( $\gamma = \beta_s/\beta_0$ ) of the blood activity can be estimated from a region over a vessel. The product of the initial blood-pool image multiplied at each point by  $\gamma$  is used to create a "predicted blood-pool" image. When this image is subtracted from  $I_s$ , the result is a difference image ( $D$ ), which represents non-blood-pool activity sources.

To generate the difference image, it was necessary to ensure that regional computations were performed on corresponding regions. The immediate and delayed images were not originally collected to ensure anatomic correspondence so it was necessary to realign the images prior to subtraction. The alignment was done by a manual process for each leg. This entailed rotations and shifts

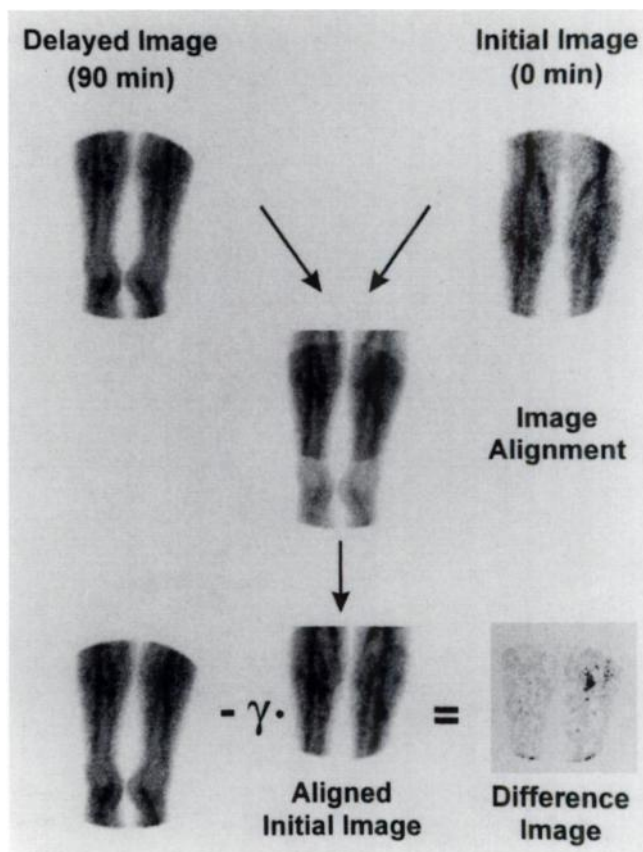


**FIGURE 2.** Image manipulations that produce the difference image. The initial and delayed images must be superimposed anatomically point for point for quantitative comparisons. Each limb in the initial image is shifted and rotated until it is anatomically congruent with the limb location in the delayed image. The aligned image is checked by rapidly alternating its display with the 90-min image (center). Once properly aligned, initial blood-pool distribution is multiplied by its fractional change factor ( $\gamma$ ) and subtracted from the 90-min delay image to produce the difference image. The hot spot remaining in the difference image represents a venogram positive thrombus in the right posterior tibial vein.

of one image over the other until there was no apparent displacement when the image pairs were viewed in a rapidly alternating sequence. Figure 2 shows a pair of images with discordant patient positioning. After each limb in the initial image was independently shifted and rotated to correspond to its subsequent position, the composite aligned initial image ( $I_0$ ) was multiplied by  $\gamma$  and subtracted from the 90-min image ( $I_s$ ) to produce the difference image. The  $\gamma$  factor was estimated by defining a region over the vessels in the aligned composite initial image ( $\beta_0$ ) and taking the ratio of the sum of counts in this zone to the corresponding pixel activity in the 90-min image ( $\beta_s$ ).

### Readers and Interpretation Studies

Image evaluation methods were tested on seven novice readers using receiver operating characteristic (ROC) analyses. The readers were selected from a population of medical personnel, students and radiology residents. The images were presented at random from the study file. Each reader was trained in a standardized fashion using written descriptions of the interpretive strategies appropriate to original T2G1s and difference images. All measures

of performance were based on a limb site analysis and not on overall patient study diagnosis.

Interpretation studies were carried out as follows. Novice readers were given an anatomic diagram of the deep venous system and were asked to refer to it in reading both the original T2G1s images and the difference images. For the original data, the readers were instructed to compare the 0- and 90-minute image in each vascular region. They were asked to seek vascular sites that increased in intensity relative to contralateral or neighboring vascular segments. They were cautioned that dilated vessels may show regions of increased activity that do not enhance with time. They were also instructed to compare similar regions of the leg and make sure that they mentally corrected for shift, rotation, and intensity differences between images before making interpretations. For the difference images, the novice readers were informed that clots have high relative intensity and occur in the distribution of the deep venous system. For both methods, readers were cautioned not to consider any uptake in superficial veins or in soft tissues unrelated to deep venous vessels as positive for DVT.

Software was written for a personal computer to present the images on a high-resolution (1024 × 768 super VGA) color monitor and to collect interpretation data. Image intensity and color scale mappings were freely adjustable. Readers were trained in the manipulation of image data and color bar tools. The contrast and background erase for each image could be set independently. The readers were encouraged to adjust the images as needed to compare the data. For three of the seven novice readers, the relative intensities of the images were initially set according to a prechosen "optimum" as judged by an experienced reader who was unblinded to the venogram results (BRL). The other four readers were presented with images that were adjusted so the image data values covered the full range of the display.

Readers were trained for each interpretation method immediately prior to viewing the images. The readers were given two example studies (one normal and one abnormal) and were encouraged to read each in the presence of the trainer and to ask any questions regarding the use of the software. The readers were then asked to interpret 250 limb sites using either original (0- and 90-min) T2G1s image pairs or the difference image. Each limb was inspected and rated as to the likelihood of the presence of a clot in the deep venous system. Likelihood statements were recorded in one of five categories (definite positive, probably positive, uncertain, probably negative and definite negative). No case histories were provided and images associated with each method were presented in random order. Readers were required to finish reading all images for each method in one sitting. Interpretation sessions were performed on sequential days in a dedicated low light level room. The order of method testing was determined by coin toss.

The results of the interpretation studies were plotted as ROC curves (9). All ROC analyses and comparisons were performed using ROC software provided by Charles Metz for the personal computer (10,11). ROC curve fitting was performed with ROCFIT for single ROC curve data and CORROC2 was used for ROC curve comparisons. The area under the ROC curve ( $A_z$ ) was used as a measure of the overall accuracy of each method of image evaluation (12).

## RESULTS

Selected images from the T2G1s antifibrin multicenter study in patients with DVT are shown in Figure 3. Three

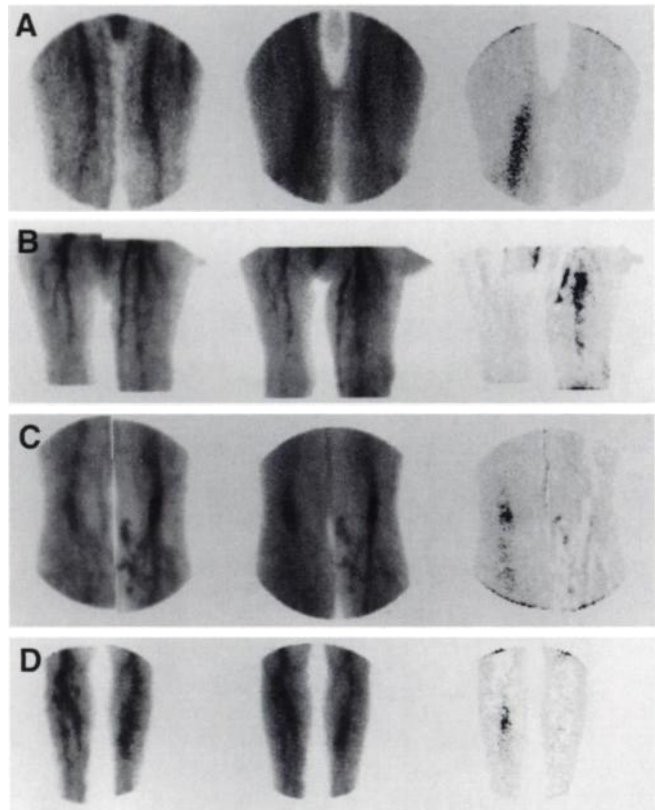


**FIGURE 3.** Selected images from the set of scans interpreted by novice readers. (A) Thrombus of right anterior thigh. In the immediate view, the distal portion of the right superficial femoral vein demonstrates a deficit in blood-pool activity which corresponds to the site of intense localization of tracer in the 90-min image. The difference image shows intense localization of activity in the right thigh in the area of the right superficial femoral vein. The contrast venogram also was evaluated as positive for acute DVT in the right thigh. Doppler/B-mode imaging did not detect acute DVT in this patient. (B) Thrombus of left anterior thigh. Immediate view shows an area of decreased activity in the left superficial femoral vein, which at 90 min demonstrates intense localization of antibody. There is corresponding intense uptake in the upper left thigh in the difference image. The venogram was positive for acute DVT. (C) Possible thrombus of the left posterior knee. In the immediate view, left popliteal demonstrates lower activity than the right. The difference image shows a concentrated area of intense uptake in the left popliteal. The venogram in this case was adjudicated to be indeterminate for acute DVT in the left knee. (D) Venogram negative study of the left calf. The T2G1s study was interpreted as positive for DVT in the left calf by the multicenter trial expert reader panel. The difference image shows concentrated and intense uptake in the area of the left peroneal vein. The venogram of the left calf was evaluated by one radiologist as negative, by another as indeterminate and by a third as positive for acute DVT in the peroneal vein.

images are shown in each set. The image on the left is the immediate blood pool obtained within 10 min of antibody injection. The middle image is obtained at approximately 90 min after injection, and the image on the right is the difference analysis. The immediate image has been realigned so that it spatially corresponds to the location of the 90-min image. The difference image shows the distribution of all non-blood-pool activity. Some of the tracer in the

**TABLE 1**  
Comparison of Scan Interpretation Accuracy and Interpretation Time for Novice Readers in Studies without Intensity and Contrast Adjustment

| Reader <sup>‡</sup> | A <sub>z</sub> ROC Area* |                   | Interpretation Time <sup>†</sup> |            |
|---------------------|--------------------------|-------------------|----------------------------------|------------|
|                     | Unprocessed              | Difference        | Unprocessed                      | Difference |
| A                   | 88.4                     | 94.5              | 9.2                              | 3.7        |
| B                   | 77.0                     | 87.6 <sup>§</sup> | 26.9                             | 12.8       |
| C                   | 76.3                     | 88.9 <sup>§</sup> | 21.8                             | 6.5        |
| D                   | 75.0                     | 91.7 <sup>§</sup> | 11.9                             | 6.3        |
| mean                | 79.1                     | 90.7 <sup>§</sup> | 17.4                             | 7.3        |

\*Area under the ROC curve as a percent of total area.

<sup>†</sup>Average time for limb site interpretation by each modality.

<sup>‡</sup>Readers A–D read images with no intensity adjustment. Readers E–G read images with intensities adjusted to provide the best reference for detecting thrombi.

<sup>§</sup>Significant difference between areas under ROC curve for unprocessed and difference images.

**TABLE 2**  
Comparison of Scan Interpretation Accuracy and Interpretation Time for Novice Readers in Studies with Intensity and Contrast Adjustment

| Reader <sup>‡</sup> | A <sub>z</sub> ROC Area* |            | Interpretation Time <sup>†</sup> |                   |
|---------------------|--------------------------|------------|----------------------------------|-------------------|
|                     | Unprocessed              | Difference | Unprocessed                      | Difference        |
| E                   | 91.7                     | 93.5       | 25.7                             | 6.9               |
| F                   | 83.0                     | 83.5       | 12.6                             | ND <sup>¶</sup>   |
| G                   | 90.9                     | 89.4       | 19.6                             | 9.8               |
| mean                | 88.5                     | 88.8       | 22.7 <sup>**</sup>               | 8.3 <sup>**</sup> |

\*Area under the ROC curve as a percent of total area.

<sup>†</sup>Average time for limb site interpretation by each modality.

<sup>‡</sup>Readers A–D read images with no intensity adjustment. Readers E–G read images with intensities adjusted to provide the best reference for detecting thrombi.

<sup>§</sup>Significant difference between areas under ROC curve for unprocessed and difference images.

<sup>¶</sup>Not determined.

<sup>\*\*</sup>Mean of two readers E, G.

difference image is due to transvascular leak of the Fab' molecule (13).

Under the circumstance where the test images were presented without preoptimized image intensity and contrast, novice readers were most accurate using the difference image (Table 1). If raw T2G1s antifibrin image intensity and contrast were set to facilitate comparison between initial blood-pool and delayed images, novice readers made correct interpretations using either raw T2G1s images or the difference image (Table 2). The area under the ROC curve (A<sub>z</sub>), a measure of method accuracy, was significantly different ( $p < 0.05$ ) for three of the four readers with no intensity optimization [mean A<sub>z</sub> of 79.1% (raw) and 90.7% (difference), Fig. 4A–D)]. Three readers whose images were optimized showed ROC curve areas of 88.5% for the raw images and 88.8% for the difference analysis image ( $p = ns$ , Fig. 4E–G). Average diagnostic decision time for all readers, per limb site, was  $18.2 \pm 7.8$  sec, mean  $\pm$  s.e.m., (raw) and  $7.6 \pm 4.6$  sec (difference).

## DISCUSSION

Thromboembolic disease has an estimated incidence of 2.5 million cases per year in the United States (14). Nearly 20% of all hospitalized patients develop DVT or pulmonary embolization (PE). Unfortunately, only half of patients with confirmed DVT show clinical evidence of thrombosis, and only a third of patients with symptoms compatible with DVT actually have the disease. Although over 90% of pulmonary emboli arise from the deep venous system, clinical symptoms of DVT occur in as few as 20% of patients with PE (15). Given the morbidity and mortality associated with PE, accurate detection of DVT is of great clinical concern.

Radiolabeled monoclonal antibodies that bind to fibrin may provide an imaging technology that is highly specific and sensitive for DVT (3). The antifibrin T2G1s antibody is directed against an epitope that becomes inaccessible be-

cause of fibrin crosslinking or is removed by the action of plasmin and is therefore available for binding only on fibrin in newly-formed, acute venous thrombi (4).

### Blood-Pool Background and Clot Detection

Blood-pool activity is a major problem in thrombus detection. Prominent localizations suggestive of thrombi may be due to nonspecific blood-pool activity in dilated vessels. Furthermore, clot detection is more difficult where activity in surrounding blood or soft tissue obscures thrombus uptake. As with other tracer imaging procedures, successful target detection with antifibrin is a function of the ratio of target signal-to-background noise (16–18). Nevertheless, a target-to-background ratio  $>1$  may not be necessary to achieve clinical utility. For example, in the large, well-controlled, multicenter trial of the clinical safety and effectiveness of T2G1s anti-fibrin, images were evaluated when blood-pool background was high. Despite this, a panel of experienced readers were able to detect acute deep venous thrombi with better than 75% accuracy, sensitivity and specificity relative to contrast venography which was used as the diagnostic gold standard. The strategy used by the panel entailed comparison of initial blood-pool distribution and the delayed (90-min, 4–6-hr) uptake patterns. The diagnostic criteria for positive studies were based on the changes in regional activity, not the magnitude of tracer uptake. The rationale for this is based on the presumption that nonspecific blood-pool activity should decrease with time, whereas sites with thrombi should show increasing tracer activity (8). It is apparent from this experience and from prior observations in immunoscintigraphy of tumors (19,20) that high background in images does not preclude interpretation as long as sequential images provide information on the dynamics of tracer distribution.

To identify a vascular zone that has increasing activity over time, it must be contrasted to a reference region that contains only blood-pool and soft-tissue background activ-

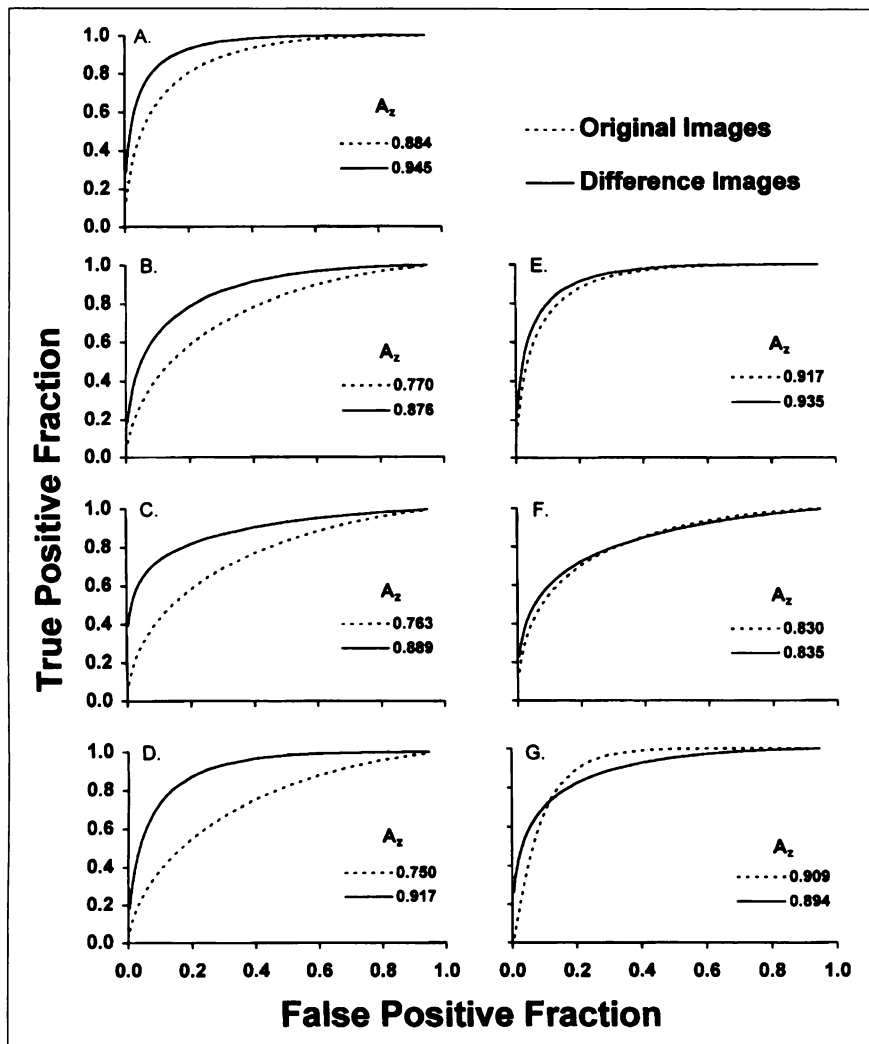


**FIGURE 4.** Plots of ROC results comparing interpretation accuracy of novice readers examining the original image set compared to the difference image set. The mean of the areas under the ROC curve ( $A_z$ ) for four readers whose images were not optimized (plots A–D) was 79.1% for the original and 90.7% for the difference images ( $p < 0.05$ ). Plots E–G are the results from three readers whose image sets were preset to optimum contrast and intensity levels. The mean  $A_z$  for these readers was 88.5% for the original images and 88.8% for the difference images ( $p = ns$ ).

ity. The comparison can be influenced by differences in shifts in limb position, temporal variation in tracer biodistribution, general image intensity or count density. These factors can be taken into account as part of the decision process for each vascular segment, but they increase the complexity of the interpretation process. Quantitative analysis of the image pairs reduces the number and complexity of the image comparisons required to detect thrombi. The first step of the process, image alignment, obviates errors from discordant region comparisons. The single image produced by the difference operation minimizes the influence of image intensity in interpretation. The difference image reflects non-blood-pool activity, the important information in thrombus detection.

#### Novice Reader Performance Studies

Novice readers were used in difference image assessment to minimize the effect of skills that more sophisticated readers might bring to the evaluation sessions. We tried to minimize other sources of bias by using a single trainer working from a standard set of materials and instruction techniques for all subjects. Preliminary tests of the instructional techniques showed that novices required a clear understanding

of the anatomy of the deep venous system to make accurate interpretations. A number of interpretation errors were caused by hot spots that were related to thrombosis in superficial veins or were due to nonthrombotic uptake in soft-tissue sites related to trauma, surgery, infection and inflammation.

The ROC data suggest that novice readers make a high percentage of correct interpretations of T2G1s images using either of the methods we tested. The results of the ROC analysis also suggest, however, that accuracy of thrombus detection by novice readers is affected by the complexity of the decision task. The readers whose original T2G1s images were intensity optimized had better accuracy than readers using unadjusted images. This suggests that choosing the best intensity for comparison is not easy for novice readers. When using the difference analysis images, intensity factors are much less important because no inter-image comparisons are required. The time required by readers to make interpretations was used as a measure of the difficulty or complexity of the decision process. On average, the original images required 2.4-fold more time to evaluate, a difference which was presumably due to the greater number of

comparisons and decisions required to interpret the original image pairs. Conversely, the raw T2G1s images were superior to the difference image with regard to preserving the anatomic detail of the deep venous system. The difference analysis often eliminated much of the image structure and made it difficult to determine the location of enhancing regions. Although our studies do not examine the value of using raw images and difference images together, an additional improvement in reader accuracy may result from their combined use.

#### Technical Aspects of Difference Analysis

The difference equations (see Appendix) indicate that this process may be applied to comparisons of an initial image and any single delayed image. It may also be applied to an initial image and any combination or sequence of delayed images compared as an aggregate image. For example, a single initial blood-pool image could be compared to an integrated image containing all subsequent data collected for any time that is practical to the imaging setting. Such integration would increase the statistical accuracy of characterizations of nonblood-pool sources of activity.

To compare an initial image to subsequent data, the images must be aligned so that anatomical congruence is maintained. The visual alignment process appears satisfactory to correct for spatial translation and in-plane limb rotation relative to the gamma camera. It is not possible to correct for out-of-plane rotation or axial limb rotation, but fortunately these motions do not occur to any significant extent. The supine position of the patient on an imaging table eliminates out-of-plane limb rotation, i.e., angulation toward, or away from, the camera. Axial rotation did not often occur, presumably because of the natural tendency of gravity to settle the limb at the same relaxed position. Although image registration was required in this retrospective analysis, in prospective situations, most alignment problems can be avoided by care taken at the time of image collection.

#### CONCLUSION

We have described procedures for comparing sequential images of  $^{99m}\text{Tc}$  antifibrin monoclonal antibody that appear to enhance novice reader accuracy and confidence in detecting deep venous thrombi. Difference analysis takes advantage of the relatively unique circumstances presented by the fibrin thrombus, i.e., the target is intravascular. An intravascular target is located within the vascular space or on the vessel wall. To localize at these sites, tracer does not need to diffuse into the extravascular space but can interact immediately with the target. For the same reason, background noise from extravascular tissues can be avoided. Most tracers must migrate from the blood to localize at an extravascular target. Unfortunately, difference analysis is not likely to be useful for extravascular targets. Because of the number of tissue compartments involved, it is very difficult to remove the activity from the extravascular space using quantitative techniques.

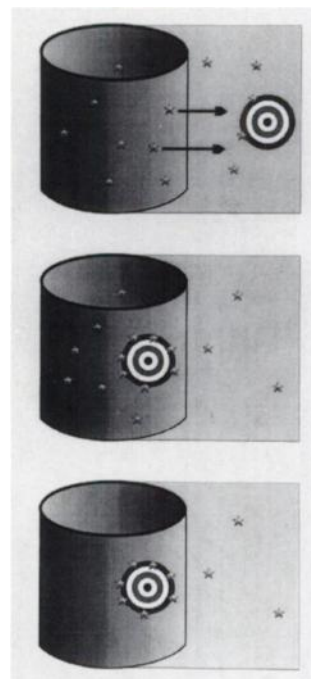


**FIGURE 5.** (A) Extravascular targeting. The tracer must leave the vessel to interact with the tissue target site. Diffusion into healthy tissue in nonaffected areas of the body occurs as well. Sufficient time must pass for this nonspecific tissue background activity and remaining blood-pool activity to clear for adequate visualization of the target site. (B) Intravascular targeting. The tracer can interact immediately with the vascular target site. Despite potentially rapid and intense localization at the target, however, the target itself resides within the area of highest background activity, i.e., the blood pool. (C) Intravascular targeting/subtraction imaging. Subtraction of blood-pool activity from an image with a vascular target effectively removes the source of the greatest background interference and enhances the detection of the target site. The ability to remove blood-pool activity quantitatively, at any point in time, rather than relying on physical clearance may allow for shorter imaging times.

Fortunately, the problem of background elimination is fundamentally different for targets that are intravascular (Fig. 5). Because the blood-pool is a single, well-mixed compartment, its activity can be quantitatively analyzed and subtracted. When targets are intravascular and the tracer molecule remains within the blood, there may be no advantage to physically clearing blood-pool activity that would otherwise be available to combine with the target. Fibrin, neovascular antigens and endothelial selectins are examples of molecules which may be targeted directly because they lie within, or adjacent, to the blood pool. These intravascular targets may provide significant opportunities to improve the accuracy of disease detection.

#### APPENDIX

Let there be a region of interest,  $\beta$ , representing blood-pool activity defined on a series of images from  $I_0$  to  $I_n$ . Define a difference image,  $\delta_i$  in which each pixel is the difference between corresponding pixels in  $I_i$  and  $\gamma_i I_0$ ,  $\gamma_i$  representing the fractional change in the activity of the blood pool,  $\beta_i/\beta_0$ . An aggregate

difference image, D, may also be defined as the sum of one or more  $\delta_i$ :

$$D = \sum_{i=a}^b \delta_i = \sum_{i=a}^b (I_i - \gamma_i I_0) = \sum_{i=a}^b I_i - I_0 \sum_{i=a}^b \gamma_i$$

or

$$D = \sum_{i=a}^b I_i - I_0 \sum_{i=a}^b \frac{\beta_i}{\beta_0}$$

and rewriting using

$$I_s = \sum_{i=a}^b I_i, \beta_s = \sum_{i=a}^b \beta_i, \gamma_s = \beta_s / \beta_0$$

we have

$$D = I_s - \gamma_s I_0. \quad \text{Eq. A1}$$

The s. d.  $\sigma_s$  of the difference image D due to counting fluctuations in  $I_s$ ,  $I_0$  and  $\gamma_s$  is found using the error propagation rule:

$$\sigma_u^2 = \left(\frac{\partial u}{\partial x_1}\right)^2 \sigma_{x_1}^2 + \left(\frac{\partial u}{\partial x_2}\right)^2 \sigma_{x_2}^2 + \dots \quad \text{or}$$

$$\sigma_D^2 = \left(\frac{\partial D}{\partial I_0}\right)^2 \sigma_{I_0}^2 + \left(\frac{\partial D}{\partial I_s}\right)^2 \sigma_{I_s}^2 + \left(\frac{\partial D}{\partial \gamma_s}\right)^2 \sigma_{\gamma_s}^2 \quad \text{Eq. A2}$$

substituting partials of D with respect to  $I_s$ ,  $I_0$  and  $\gamma_s$ :

$$\left(\frac{\partial D}{\partial I_s}\right)^2 = 1, \left(\frac{\partial D}{\partial I_0}\right)^2 = \gamma_s^2, \left(\frac{\partial D}{\partial \gamma_s}\right)^2 = I_0^2$$

into Equation A2 and since

$$\sigma_{I_s}^2 = I_s, \sigma_{I_0}^2 = I_0$$

we have

$$\sigma_D^2 = I_s + \gamma_s^2 I_0 + I_0^2 \sigma_{\gamma_s}^2. \quad \text{Eq. A3}$$

Re-application of the error propagation rule to the equation for  $\gamma_s$  produces:

$$\sigma_{\gamma_s}^2 = \left(\frac{\partial \gamma_s}{\partial \beta_s}\right)^2 \sigma_{\beta_s}^2 + \left(\frac{\partial \gamma_s}{\partial \beta_0}\right)^2 \sigma_{\beta_0}^2 \quad \text{or} \quad \sigma_{\gamma_s}^2 = \left(\frac{1}{\beta_0}\right)^2 \sigma_{\beta_s}^2 + \left(\frac{-\beta_s}{\beta_0^2}\right)^2 \sigma_{\beta_0}^2$$

Rearranging using

$$\sigma_{\beta_s}^2 = \beta_s, \sigma_{\beta_0}^2 = \beta_0$$

we have

$$\sigma_{\gamma_s}^2 = \gamma_s^2 (1/\beta_s + 1/\beta_0)$$

which when substituted back into Equation A3 yields:

$$\sigma_D = \sqrt{I_s + \gamma_s^2 I_0 (1 + I_0 (1/\beta_s + 1/\beta_0))}. \quad \text{Eq. A4}$$

## ACKNOWLEDGMENTS

The authors thank the principal investigators of the study sites involved in the collection of the multicenter Phase I and II trials of  $^{99m}\text{Tc}$ -T2G1s and Centocor Inc. staff who provided access to the data. The authors are indebted to Michael V. Green for the error analysis of the difference image. Bruno and Steven Caridi provided essential support in reader data collection and image processing.

## REFERENCES

- Dalen JE, Alpert JS. Natural history of pulmonary embolism. *Prog Cardiovasc Dis* 1975;17:259-270.
- Morrell MT, Dunnill MS. The post-mortem incidence of pulmonary embolism in a hospital population. *Br J Surg* 1968;55:347-352.
- Knight LC. Imaging thrombi with radiolabelled anti-fibrin monoclonal antibodies. *Nucl Med Commun* 1988;9:823-829.
- Kudryk B, Rohoza A, Ahadi M, Chin J, Wiebe ME. Specificity of a monoclonal antibody for the NH2-terminal region of fibrin. *Mol Immunol* 1983; 20:1191-1200.
- Schaible TF, Alavi A. Antifibrin scintigraphy in the diagnostic evaluation of acute deep venous thrombosis. *Semin Nucl Med* 1991;21:313-324.
- Knight LC, Maurer AH, Ammar IA, et al. Technetium-99m-antifibrin Fab' fragments for imaging venous thrombi: evaluation in a canine model. *Radiology* 1989;173:163-169.
- Rosebrough SF, McAfee JG, Grossman ZD, et al. Thrombus imaging: a comparison of radiolabeled GC4 and T2G1s fibrin-specific monoclonal antibodies. *J Nucl Med* 1990;31:1048-1054.
- Schaible T, Dewoody K, Weisman H, Line B, Keenan A, Alavi A. Accurate diagnosis of acute deep venous thrombosis with technetium-99m antifibrin scintigraphy: final phase III trial results [Abstract]. *J Nucl Med* 1992; 33(suppl):848.
- Swets JA, Pickett RM. *Evaluation of diagnostic systems: methods from signal detection theory*. New York: Academic Press; 1982.
- Metz CE. ROC methodology in radiologic imaging. *Invest Radiol* 1986;21: 720-733.
- Metz CE. Some practical issues of experimental design and data analysis in radiological ROC studies. *Invest Radiol* 1989;24:234-245.
- Hanley JA, McNeil BJ. The meaning and use of the area under a receiver operating characteristic (ROC) curve. *Radiology* 1982;143:29-36.
- Line BR, Herrmannsdoerfer AJ, Battles AH, Weber PB, Dansereau RN, Blumenstock FA. Premortem biodistribution of radioactivity in the rat: measurement of blood and tissue activity of tracers used in clinical imaging studies. *Lab Animal Sci* 1994;44:495-502.
- Sherry S. The problem of thromboembolic disease. *Semin Nucl Med* 1977; 7:205-211.
- Browse NL, Lea Thomas M. Source of nonlethal pulmonary emboli. *Lancet* 1974;1:258.
- Rockoff SD, Goodenough DJ, McIntire KR. Theoretical limitations in the immunodiagnostic imaging of cancer with computed tomography and nuclear scanning. *Cancer Res* 1980;40:3054.
- Halpern SE, Dillman RO. Problems associated with radioimmunodetection and possibilities for future solutions. *J Biol Response Mod* 1987;6:235-262.
- Goldenberg DM. Current status of cancer imaging with radiolabeled antibodies. *J Cancer Res Clin Oncol* 1987;113:203-208.
- Britton KE, Granowska M, Mather SJ. Radiolabeled monoclonal antibodies in oncology. I. Technical aspects. *Nucl Med Commun* 1991;12:65-76.
- Granowska M, Nimmon CC, Britton KE, et al. Kinetic analysis and probability mapping applied to the detection of ovarian cancer by radioimmunoscintigraphy. *J Nucl Med* 1988;29:599-607.